01 Aug 2018

A New Approach to Measure Soil Shrinkage Curve

Lin Li

Xiong Zhang
Missouri University of Science and Technology, zhangxi@mst.edu

Recommended Citation

L. Li and X. Zhang, "A New Approach to Measure Soil Shrinkage Curve," *Geotechnical Testing Journal*, vol. 42, no. 1, ASTM International, Aug 2018.
The definitive version is available at https://doi.org/10.1520/GTJ20150237

Geotechnical Testing Journal

doi:10.1520/GTJ20150237 / Vol. 42 / No. 1 / 2019 / available online at www.astm.org

Lin Li[1] and Xiong Zhang[2]

A New Approach to Measure Soil Shrinkage Curve

Reference

Li, L. and Zhang, X., "A New Approach to Measure Soil Shrinkage Curve," *Geotechnical Testing Journal*, Vol. 42, No. 1, 2019, pp. 1–18, https://doi.org/10.1520/GTJ20150237. ISSN 0149-6115

ABSTRACT

The shrinkage curve is widely used to characterize soil deformation during drying. Over the years, several methods have been developed to measure soil shrinkage curves. However, these methods suffered from several limitations and were rarely used because of difficulties in accurate soil volume measurement during drying. In this study, a simple method is proposed to measure soil shrinkage curves. The soil volume is measured using a photogrammetric technique from which a three-dimensional (3D) model of the soil specimen during drying can be accurately reconstructed. The soil volume is calculated based on the reconstructed 3D model. Meanwhile, a digital balance is used to record the soil weight for the back-calculation of soil water content, which will be used for the shrinkage curve construction. The overall volume measurement error was evaluated to be 0.35 % and 0.43 % through tests on aluminum cylinders and a saturated soil, respectively. With the proposed method, a series of tests were performed to measure the shrinkage curves of a soil mixture (i.e., Fairbanks silt and Kaolin at a ratio of 1:1). Results from these shrinkage tests indicate that the proposed method is cost-effective, accurate, and reliable for soil shrinkage curve measurements.

Keywords

shrinkage curve, volume change, photogrammetry, three-dimensional reconstruction

Manuscript received October 4, 2015; accepted for publication February 9, 2018; published online August 20, 2018.

[1] School of Civil Engineering, Nanjing Forestry University, 159 Longpan Rd., Nanjing 210037, China (Corresponding author), e-mail: lli10@alaska.edu, https://orcid.org/0000-0002-0950-8412

[2] Civil, Architectural and Environmental Engineering, Missouri University of Science and Technology, Rolla, MO 65409-0030, USA

Introduction

The shrinkage curve, which defines the relationship of soil volume and moisture content during drying, is widely used to evaluate the shrinkage, crack development, and swelling potentials of earthwork, especially when cohesive soils are involved. As stated in Fredlund

and Houston (2013), Fredlund and Zhang (2013), and Cornelis et al. (2006), the shrinkage curve also played an important role in the interpretation of soil water retention curve data, and shrinkage curve measurement should be used in combination with the soil water retention curve. To characterize the soil shrinkage behavior, simultaneous measurements of soil volume and water content are required. The soil water content can be simply measured using a balance. However, measuring the soil shrinkage curve is still a great challenge for engineers, because of the difficulties in accurate soil volume measurement during testing.

To date, there is no American Society for Testing and Materials (ASTM) standard available for soil shrinkage curve measurement. ASTM D4943, *Standard Test Method for Shrinkage Factors of Soils by the Wax Method*, and ASTM D427, *Standard Test Method for Shrinkage Factors of Soils by the Mercury Method*, can only be used to determine the soil shrinkage limit (SL). Also, both methods suffer from safety concerns due to the use of wax and mercury for volume measurement. To accurately predict the soil volume at different water contents, a complete shrinkage curve is usually required instead of the SL.

Many research efforts have been dedicated to accurately measure the soil shrinkage curves (Brasher et al. 1966; Schafer and Singer 1976; Berndt and Coughlan 1977; Reeve, Hall, and Bullock 1980; McGarry and Daniells 1987; Sibley and Williams 1989; Kim et al. 1992; Tariq and Durnford 1993; Crescimanno and Provenzano 1999; Braudeau et al. 1999; Krosley, Likos, and Lu 2003; Cornelis et al. 2006; Boivin 2007; Sander and Gerke 2007; Huang, Shao, and Tan 2011; Stewart et al. 2012; Bensallam et al. 2012; Lu and Kaya 2013; Hobbs et al. 2014; and Jain, Wang, and Fredlund 2015). The volume change measurement can be broadly classified into the contact and noncontact methods.

CONTACT METHODS

The simplest method to measure the volume of a soil cylinder is performed through direct sample height and diameter measurements, as presented in Schafer and Singer (1976), Berndt and Coughlan (1977), Huang, Shao, and Tan (2011), and Fredlund and Houston (2013). However, this method can only be applied on regular specimens prepared by molding, lathing, slicing, or coring. The measurement accuracy can also be low, especially when the soil regularity is lost as drying proceeds. In Boivin (2007) and Bensallam et al. (2012), the deformation of soil cylinders during wetting and drying was monitored using a displacement transducer. To calculate the soil volume change, the diameter of the soil cylinder was assumed to be constant, which might not be consistent with the real soil deformation.

Besides the direct height and diameter measurement method, Archimedes' law was also reported to be used to measure the soil volume during the shrinkage test, as presented in Brasher et al. (1966), Reeve, Hall, and Bullock (1980), Sibley and Williams (1989), Bronswijk (1990), and Krosley, Likos, and Lu (2003). In these studies, different materials, such as saran resin and glue, or displaced fluid such as toluene, were adopted to coat the soil for volume measurement. The major advantage of this method was its applicability to soil clods with random shapes. However, it was found that the coating material did not properly make contact with the soil clod. This method was also subjected to errors from water penetration and the presence of air bubbles.

In Tariq and Durnford (1993) and Cornelis et al. (2006), soil volume change during drying was measured using a balloon method. The soil to be tested was oven-dried, pulverized, and then mixed with water in a rubber balloon. Soil volume change was also measured based on Archimedes' law. Since the soil is required to be oven-dried and sieved before testing, this method is not applicable to in situ soil samples.

NONCONTACT METHODS

Noncontact methods are more attractive than contact methods, since they are nondestructive to the soil samples. In Braudeau et al. (1999), a retractometer was used for continuous sample height and diameter measurements during a shrinkage test with the help of several laser sensors. A similar test apparatus was also reported to be used as presented in Hobbs et al. (2014). With the increasing availability of inexpensive digital cameras, image-based methods are getting popular for soil shrinkage curve measurement (e.g. Puppala, Katha, and Hoyos 2004; Sander and Gerke 2007; Stewart et al. 2012; Puppala, Manosuthikij, and Chittoori 2013; Lu and Kaya 2013; and Jain, Wang, and Fredlund 2015).

Puppala, Katha, and Hoyos (2004) and Puppala, Manosuthikij, and Chittoori (2013) proposed digital imaging technology to measure the volumetric strain of expansive soils subjected to a drying process. To measure the volumetric strain of a compacted cylindrical specimen, several images were captured for the top, bottom, and side surfaces before (i.e., initial state) and after (i.e., final state) the drying process. The obtained images were processed to determine the cross-section and side surface (with consideration of the cracks) areas of the specimen in pixels. The ratios (i.e., final/initial) of the cross-section and side surface were then used to calculate the overall soil volumetric strain. In this method, the volumetric strain calculation with consideration of the cracks was problematic, since the crack width could vary with depth in the soil. As a result, this method provided consistently higher volumetric strains than the manual measurement using a caliper.

In Sander and Gerke (2007), a three-dimensional (3D) optical scanning device that consisted of a black-and-white camera and a white-light projector was used to assess the geometry of soil clods during drying. The clod was mounted on a tripod to facilitate the volume measurement. Coded light on the soil clod from the projector was captured by the camera at different times. A point cloud, which represented the soil clod surface, was then reconstructed based on the captured images and triangulated for volume calculation. The measurement result was in agreement with the coating method. However, for this method, so it could be mounted on a tripod for 3D scanning, the soil was required to be strong enough to hold itself on the tripod during drying. As a result, the obtained shrinkage curve was usually incomplete, because of the missing part of the curve when the soil was saturated or close to saturation. To reconstruct the 3D model of the soil clod, some erratic points, which were inevitably created during surface reconstruction, must be removed. The removal of these erratic points is subjective and could influence the volume measurement accuracy.

Besides these, Stewart et al. (2012) proposed a "Clodometer" method using a digital camera and a series of free software for data processing. The volume calculation was similar to the method presented in Sander and Gerke (2007). However, for this "Clodometer" method, to obtain the volume of the soil clod, a reference object with a known volume was required for each measurement to determine the calibration coefficient. According to the results presented in Stewart et al. (2012), the volume measurement error was evaluated to range from 0.4 % to 1.6 %.

A particle image velocity (PIV) technique, originally proposed in fluid mechanics for capturing particle movement in a planar pattern (Adrian 1991), was proposed to measure soil deformation by White, Take, and Bolton (2003) and Lu and Kaya (2013). The soil volume/deformation measurement was made based on a time-sequence displacement field that was extracted using an image correlation technique. For the PIV method, in order to be used for soil volume change measurement during drying or wetting, the camera has to

be calibrated to eliminate either pincushion or barrel distortion caused by the camera lens (Zhang et al. 2015). Failure to do so would cause measurement error even though the measurements were made in the same plane, as pointed out by White, Take, and Bolton (2003). The soil surface was also required to be perfectly planar since the PIV method can only make two-dimensional (2D) measurements, as stated in Lu and Kaya (2013). In order to measure soil volume change based on 2D deformation, it is required to assume the soil deformation is uniform in all directions, which was very difficult to satisfy, as demonstrated in Lu and Kaya (2013). In addition, since the PIV method is 2D, it cannot be used to measure the volume of soil with cracks, according to Lu and Kaya (2013).

In Jain, Wang, and Fredlund (2015), a camera in conjunction with two lasers was used to measure the volume change of a soil cylinder on a turntable during continuous drying. The deformation of the cylinder side surface was measured through triangulation. The deformation of the cylinder top surface was assumed to be uniform during drying. The measurement error was evaluated to be 1 % through tests on a dummy sample. However, to apply this method, a sophisticated calibration is required before any measurement. It is also questionable to assume a uniform soil deformation, since natural soils are usually anisotropic because of the difference in vertical and lateral pressures during consolidation. As a result, the volume measurement error could be worse than 1 % when applied to soil deformation measurement during testing.

As addressed above, there is still a great need to accurately measure the soil shrinkage curves. In this study, a new method is proposed, in which the soil volume during the shrinkage test is measured using a photogrammetric technique and the soil water content is measured using a digital balance, respectively. The accuracy of the photogrammetric volume measurement was evaluated through tests on aluminum cylinders and a saturated soil specimen. In addition, to demonstrate the performance of the proposed method, a series of shrinkage tests were conducted on a soil mixture with different pre-consolidation stress levels.

A Photogrammetric Volume Measurement Method

Photogrammetry is the science of making measurements from images. It has been successfully used in both laboratory and field deformation measurements (e.g. Li and Zhang 2015a, 2015b; Zhang et al. 2015; Li et al. 2016; White, Take, and Bolton 2003; Merel and Farres 1998) in the engineering field. A brief introduction on the principle of photogrammetry is presented as follows.

The principle of photogrammetry is based on triangulation using images captured by ideal pinhole cameras, typically as seen in **Fig. 1**. In the pinhole camera model, the small pinhole and the image plane correspond to the perspective center of the lens and the image sensor of a digital camera. For a 3D object, when an image is taken using this pinhole camera, a 2D image is obtained, and the depth of the object is lost as shown on the image captured at Camera Station 1 in **Fig. 1**. For the same object, its geometry appears to be different on an image captured from a different camera position (i.e., Camera Station 2) due to perspective, as shown in **Fig. 1**. If the perspective center (i.e., pinhole) of the left camera S_1 is set as the origin of an arbitrary coordinate system, there are six unknowns for the right camera orientation, as shown in **Fig. 1**, which are 3D coordinates of the

FIG. 1

Principle of photogrammetry based on pinhole camera model.

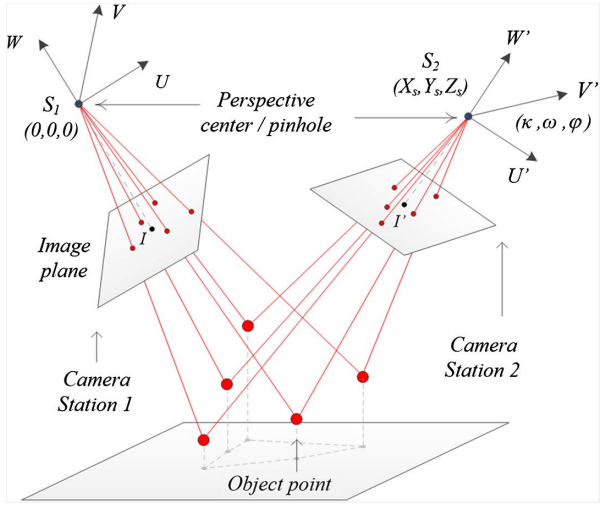

perspective center S_2 (X_s, Y_s, Z_s) and three directional angles (κ, ω, φ). The distance between any two of the five points can be measured according to the real world scale, which reduces the number of the unknowns to five. Then, five equations can be established by identifying five pairs of corresponding points on two images, based on the coplanarity of these light ray pairs. The orientation of Camera Station 2 can be determined using these equations.

Once the camera orientations are determined, for any point of interest on the object, light rays can be constructed from the corresponding perspective centers of the camera stations to the image planes. The intersection of two rays determines the 3D coordinates of the point, which is known as "triangulation" in photogrammetry. In other words, the orientation of the camera from where the images are captured is calculated using the pixel positions of the corresponding points on different images based on the pinhole camera model and principle of photogrammetry. These camera orientations, together with the images, can then be used to reconstruct the 3D geometry of the object through triangulation. The detailed principle of photogrammetry can be found in Mikhail, Bethel, and McGlone (2001).

ACCURACY EVALUATION OF THE VOLUME MEASUREMENT METHOD

In this study, a digital camera with a fixed focal length lens (in this case, a Nikon D7000 with AF-S Micro Nikkor 40 mm 1:2.8 G, Nikon, Minato, Japan) was used to capture the images for the photogrammetric volume measurement. As addressed in Zhang et al. (2015), the images captured by commercial digital cameras suffer from either pincushion or barrel distortion. However, the principle of photogrammetry is based upon the ideal pinhole camera model, which does not cause any distortion in the captured images. Therefore, the used camera set is required to be calibrated to determine the internal characteristics, such as the focal length of the camera lens, perspective center location, image sensor resolution, and radial and decentering distortion parameters, before it is used for any photogrammetric measurement. With these internal characteristics, the camera can then be idealized to a pinhole camera. Since the 1950s, several techniques have been

FIG. 2

Calibration sheet.

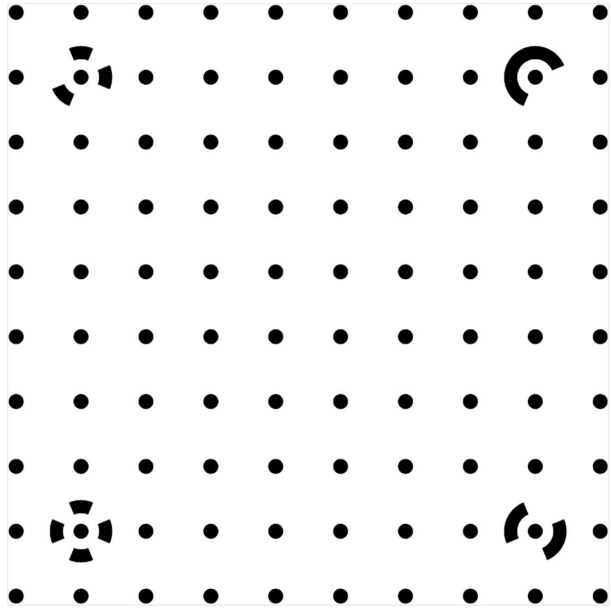

developed for camera calibration. The most popular approach is the well-established self-calibrating bundle adjustment, as presented in Triggs et al. (2000).

The camera calibration can be easily performed using several software packages, as addressed in Zhang et al. (2015). In this study, a software package (i.e., PhotoModeler Scanner from EOS Systems Inc., Vancouver, Canada) was adopted for the camera calibration. The calibration was performed by capturing 12 images of a calibration sheet, as shown in **Fig. 2**, from different view angles. With the software, the internal characteristics were then extracted based on the captured images. The calibration result is presented in **Table 1**. With the calibration results, the camera can then be idealized to a pinhole camera, as shown in **Table 1**. For this pinhole camera, all distortion parameters are equal to zero, and the principal point is located exactly at the center of the image sensor.

TABLE 1

Camera calibration results.

Parameters	Symbol	Before Idealization	After Idealization
Focal Length	f *(mm)*	41.2388	41.2388
Pixel Number	M *(pixel)*	4,928	4,928
	N *(pixel)*	3,264	3,264
Image Sensor Size	F_x *(mm)*	23.9949	24.1539
	F_y *(mm)*	15.8961	15.9964
Principal Point Coordinate	P_x *(mm)*	12.0860	12.0770
	P_y *(mm)*	7.9286	7.9982
Radial Lens Distortion	K_1 (10^{-6})	3.836	0
	K_2 (10^{-8})	−6.372	0
Decentering Lens Distortion	P_1 (10^{-6})	−6.681	0
	P_2 (10^{-5})	−1.403	0

FIG. 3

Test on aluminum cylinders: (a) aluminum cylinders and (b) setup for volume measurement.

TABLE 2

Accuracy evaluation test on aluminum cylinders.

Cylinder	Target/Caliper Measured Diameter, mm	Target/Caliper Measured Height, mm	Volume Range, mm^3	V_c, mm^3	V_p, mm^3	Error, %
1	63.5/63.50	25.4/25.42	80,297–80,582	80,503	80,557	0.07
2	63.0/63.00	24.2/24.23	75,300–75,575	75,531	75,995	0.61
3	62.5/62.51	23.0/23.04	70,430–70,696	70,709	71,222	0.73
4	62.0/62.00	21.8/21.80	65,687–65,944	65,816	65,619	−0.30
5	61.5/61.50	20.6/20.63	61,070–61,318	61,283	61,132	−0.25
6	61.0/61.00	19.4/19.44	56,576–56,816	56,813	56,896	0.15
		Mean absolute measurement error				0.35

Accuracy Evaluation Using Aluminum Cylinders

Before being used for soil volume measurement during the shrinkage test, the accuracy of the photogrammetric technique was evaluated through a test on aluminum cylinders, as shown in Fig. 3a. Table 2 summarizes the target diameter, height, and volumes of six aluminum cylinders. The machining accuracy was 0.025 mm, which corresponded to different cylinder volume ranges for six cylinders, as presented in Table 2. It should be noted that the size of the cylinders was purposely designed to be comparable to that of the soil samples for a one-dimensional consolidation test. A digital caliper was used to measure the cylinder volumes (referred to as "V_c" in Table 2). The measured volumes were within or very close to the corresponding volume ranges. To facilitate the image capturing from different view angles, as shown in Fig. 3b, the cylinder was placed on a cylindrical pedestal which rested on a turntable. Besides this, for cylinder volume calculation, a coordinate system was built using targets located on the side of the pedestal.

To accurately measure the cylinder volume, a dense point cloud which represents the cylinder surface is preferred for volume measurement. In this study, this surface reconstruction was achieved using the photogrammetric technique, with the help of texture matching between image pairs with overlaps. The texture matching, also referred as "image correlation," is typically used to measure displacements across an object surface based upon the assumption that all surfaces have their own unique textures in the form of

FIG. 4

Camera stations for image capturing.

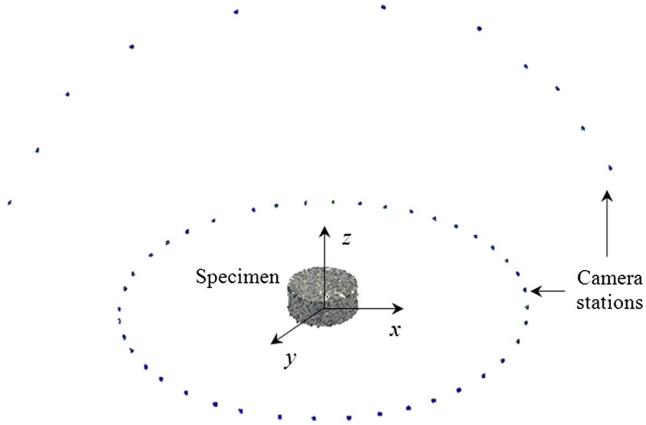

different-colored grains and the light and shadow formed between adjacent grains when illuminated (e.g. Lu and Kaya 2013; Bhandari, Powrie, and Harkness 2012; Sachan and Penumadu 2007; Rechenmacher and Medina-Cetina 2007; Lin and Penumadu 2006; Sutton et al. 2000; and Helm, McNeill, and Sutton 1996). With this technique, the correlation between images captured for the same object before and after deforming was identified, from which the soil deformation could be extracted.

To facilitate the texture matching, the surfaces of the cylinders were textured through spraying paint, as shown in Fig. 3b. The cylinder to be tested was then placed on a turntable. Before the image capturing, the turntable was turned on to rotate at a speed of 1 r/min. The images were then captured for the cylinder side surface at a fixed camera station for the soil side surface reconstruction. To obtain the volume of the cylinder, a detailed top surface was also required. This top surface reconstruction was achieved by capturing several images at camera stations above the cylinder.

The obtained images were processed using the software package PhotoModeler from EOS Systems Inc. After texture matching between image pairs, the camera stations where the images were captured were determined, as typically shown in Fig. 4, using the principle of photogrammetry. In this case, 46 images and 11 images were captured for the reconstructions of the side and top surfaces of the cylinder, respectively. A 3D coordinate system was built using the targets on the pedestal. In this coordinate system, the origin was set at the center of the pedestal top surface. The *x*-*y* plane was located at the top surface of the pedestal, which was also the bottom surface of the aluminum cylinder, as shown in Fig. 4. With the help of the texture matching technique, a point cloud that represented the top and side surfaces of the aluminum cylinder was obtained, as typically shown in Fig. 4, based on the principle of photogrammetry.

To calculate the cylinder volume, similar to the volume measurement presented in Li et al. (2016), an enclosed triangular mesh was required to be built based on the obtained point cloud. It is known that the MATLAB (MathWorks, Inc., Natick, MA) function "DelaunayTri" can be used to build triangular meshes based on points located on the same plane. However, this function was not applicable to a 3D point cloud. As a result, to facilitate the meshing, the 3D point cloud (e.g., Fig. 5a) was transformed to 2D (e.g., Fig. 5b). The transformations for the top and side surfaces were performed separately.

FIG. 5

Mesh generation: (a) obtained point cloud in 3D space, (b) transformed mesh on *x-y* plane, and (c) triangular mesh in 3D space.

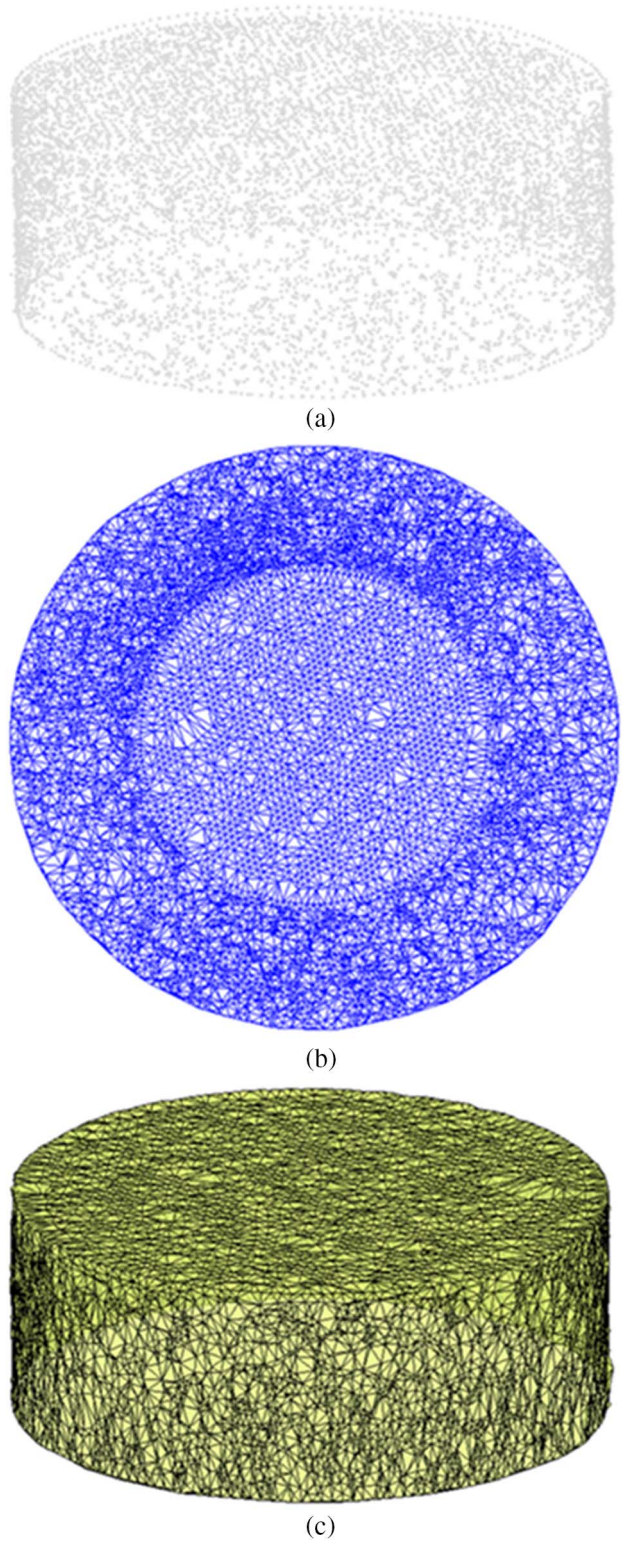

The following equations provided an example of this transformation for the points on the top and side surfaces, respectively.

$$\text{Top surface: } \begin{cases} x_{2D} = x_{3D} \\ y_{2D} = y_{3D} \end{cases} \quad (1)$$

$$\text{Side surface: } \begin{cases} x_{2D} = \left(\sqrt{x_{3D}^2 + y_{3D}^2} + (H - z_{3D})\right)\left(\frac{x_{3D}}{\sqrt{x_{3D}^2 + y_{3D}^2}}\right) \\ y_{2D} = \left(\sqrt{x_{3D}^2 + y_{3D}^2} + (H - z_{3D})\right)\left(\frac{y_{3D}}{\sqrt{x_{3D}^2 + y_{3D}^2}}\right) \end{cases} \quad (2)$$

where:

x_{2D} and y_{2D} = 2D coordinates on the *x*-*y* plane,
x_{3D}, y_{3D}, and z_{3D} = 3D coordinates in the coordinate system, and
H = cylinder height.

The top surface was directly projected onto the *x*-*y* plane, as shown in Eq 1. For the side surface, this transformation was achieved through moving the corresponding point outward in its radial direction with a distance equal to that between the point and the top surface. After this 2D transformation, a 2D triangular mesh could be easily generated using the MATLAB function (i.e., "DelaunayTri (x_{2D}, y_{2D})"), as typically shown in **Fig. 5b**. Using the same triangular mesh, the mesh for the aluminum cylinder in the 3D coordinate system was then constructed using the original 3D coordinates of the point cloud, as shown in **Fig. 5c**. To calculate the cylinder volume, a random point (e.g., the origin of the coordinate system) on the bottom surface was selected. A series of tetrahedrons were then generated by connecting this point to all the points on the cylinder surface. The volume of each tetrahedron was calculated based on the 3D coordinates of four nodes. The total volume of the cylinder was the summation of all tetrahedron volumes.

The photogrammetric measurement was performed on all six aluminum cylinders. The measured volumes "V_p" are also summarized in **Table 2**. Similar to the caliper measurement results, the measured volumes using the proposed method are within or very close to the corresponding volume ranges, which indicates that the accuracy of the proposed method is comparable to that of the digital caliper method. Compared to the target cylinder volumes, the mean absolute measurement error was calculated to be 0.35 %. Since the cylinder size is comparable to the size of the soil specimens typically used for shrinkage curve measurement, this measurement error is considered to be representative of the error of the proposed method when applied to shrinkage curve measurement.

Accuracy Evaluation Using a Saturated Soil

In addition to the test on the aluminum cylinders, an evaluation test on a saturated soil was also performed in this study. It is known that the volume change of a saturated soil is equal to the corresponding water volume/weight change. To evaluate the volume measurement accuracy of the photogrammetric method, a saturated soil specimen was prepared using a mixture of Kaolin and Bentonite at a ratio of 4:1. The soil mixture was mixed with water, as shown in **Fig. 6a**. To ensure saturation, the soil mixture was placed on a vibration table for a certain time to release the air bubbles in the soil slurry introduced during mixing. A plastic measurement target sheet, which was used to build a coordinate system, was glued to a piece of glass. The soil mixture was poured out to the target sheet. Since a textured surface was required for image matching, the soil surface was then partially covered with silt particles, as shown in **Fig. 6b**.

FIG. 6

Test on a saturated soil: (a) saturated soil mixture, (b) soil mixture covered with a thin layer of silt, (c) reconstructed soil surface, and (d) triangular mesh for volume calculation.

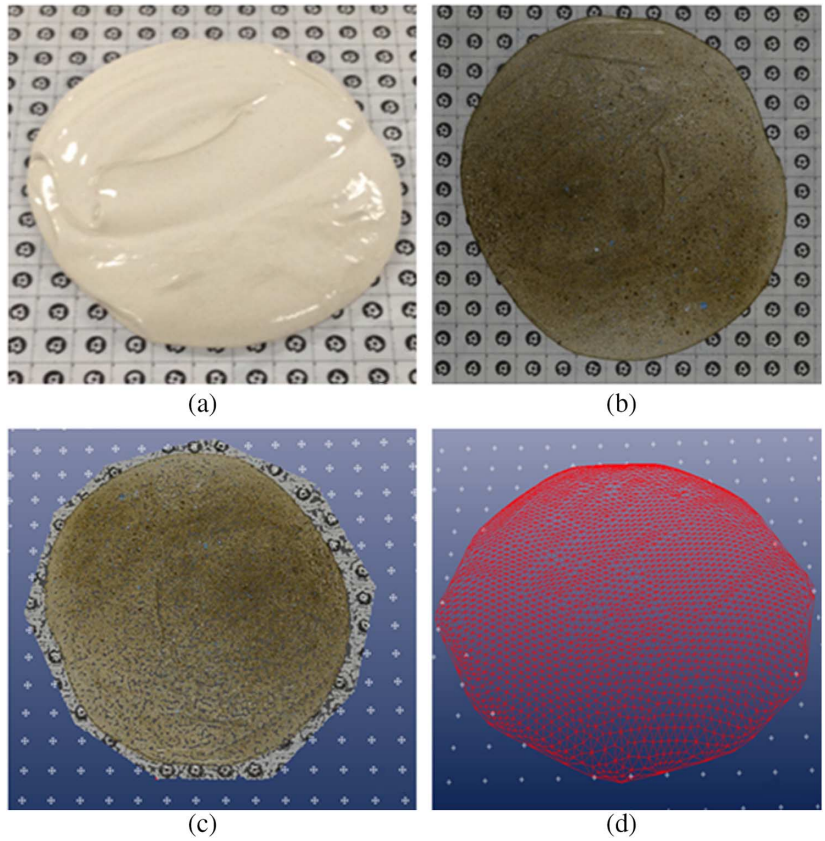

The photogrammetric method was performed to measure the initial volume of the saturated soil after this. The obtained soil surface from the photogrammetric measurement is presented in Fig. 6c. Fig. 6d shows the generated triangular mesh based on the obtained point cloud. After the initial volume measurement, the total weight of the soil was measured using a digital balance. The soil was then exposed to the atmosphere for a certain time to facilitate water evaporation. Subsequently, the soil volume was measured again, using the photogrammetric method. The drying and measuring processes were repeated until the desaturation of the soil. The soil weight and volume changes are presented in Fig. 7. The mean absolute measurement error of the proposed photogrammetric method was determined to be 0.43 %, which was close to the 0.35 % from the evaluation test on the aluminum cylinders.

Shrinkage Test

The photogrammetric method is proposed to measure the soil volume changes during the shrinkage test. To further evaluate the performance of the photogrammetric method for shrinkage curve measurement, a series of shrinkage tests on a soil mixture were also performed. The tested material was a mixture of Fairbanks silt and Kaolin at a ratio

FIG. 7

Result from the test on a saturated soil.

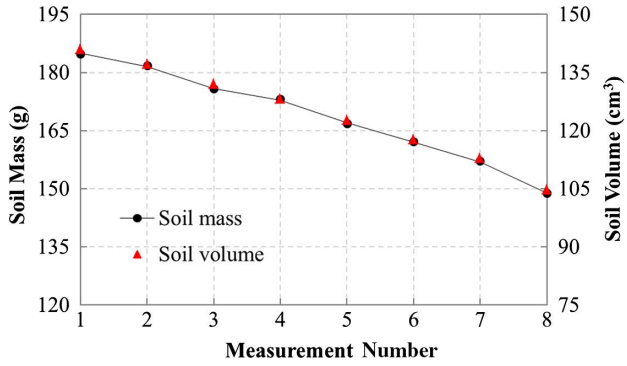

of 1:1. The liquid limit, plastic limit, and specific gravity of the soil mixture are 25.8 %, 20.0 %, and 2.75, respectively.

SPECIMEN PREPARATION

The soil mixture was oven-dried and mixed with water to the desired moisture content of 40 %, at which the soil behaved like a thick paste. The soil was then poured into a consolidation ring (25.4 mm in height and 63.5 mm in inside diameter) in an oedometer cell. Similar to the test on the saturated soil, the vibration table was also used to release the air trapped in the soil. However, in this case, it was found that it is rather difficult to release all the air in the soil, since the soil was thicker than that used for the evaluation test. As a result, the prepared soil specimens might not be fully saturated, which was later confirmed by the measurement results. Filter papers were placed at the bottom and top surfaces of the soil. The top cap of the consolidation ring was installed after this, and the oedometer cell was then filled up with water. The soil specimens were consolidated to different vertical stress levels (i.e., 12.5, 25, 50, 100, 200, and 400 kPa) using the conventional one-dimensional consolidation test apparatus. The applied vertical stress was released after the consolidation process. The soil specimens were then carefully disassembled from the oedometer cell, as shown in Fig. 8. The heights of the soil cylinders were slightly less than

FIG. 8

Shrinkage tests on saturated soils.

25.4 mm, which was the height of the consolidation ring, due to consolidation. After demolding from the consolidation ring, similar to the test on the aluminum cylinders, the soil specimens were sprayed with paint to facilitate the texture matching for soil surface reconstruction. The specimens were then ready for the shrinkage test.

SHRINKAGE TESTS

The shrinkage test was performed by exposing the soil to the atmosphere for drying. The system setup, as shown in Fig. 8b, was similar to the evaluation test on the aluminum cylinders. In this case, the soil weight variation during drying was measured using a digital balance. The images were then captured at different times, when soil weight was checked. To reconstruct the soil surface, the image capturing was the same as that for the aluminum cylinders, as shown in Fig. 4. The same mesh generation and volume calculation techniques presented in the tests on the aluminum cylinders, typically as shown in Fig. 5, were also applied to six soil specimens.

EXPERIMENTAL RESULTS

With the measurement results from the balance and the photogrammetric technique, the soil initial degree of saturation, water content and void ratio during the shrinkage test, and corresponding saturation line of the soil were determined and plotted in Fig. 9. Before drying, all soil specimens were either saturated (e.g., the soils consolidated to 100 and 400 kPa) or nearly saturated (i.e., the soils consolidated to 12.5, 25, 50, and 200 kPa). Generally, the initial void ratio of the soils decreased with increasing pre-consolidation stresses, and the initial degree of saturation of the soils increased with increasing pre-consolidation stress, which was reasonable. It should be noted that the degree of saturation of the soils consolidated to 100 and 400 kPa were slightly above 100 %, which was due to the error in soil volume measurement. As shown in Fig. 9, during drying, the soil volume continuously decreased with decreasing water content and then gradually stabilized when it reached the SL. With the obtained shrinkage curves, the corresponding SL of the tested soils were also obtained and presented in Fig. 9. It is interesting to find that the SLs of the tested soils with high pre-consolidation stress are slightly higher than those with low pre-consolidation stress. The void ratio of the tested soil mixtures during drying varied from

FIG. 9

Shrinkage test results plotted on the *w-e* plane.

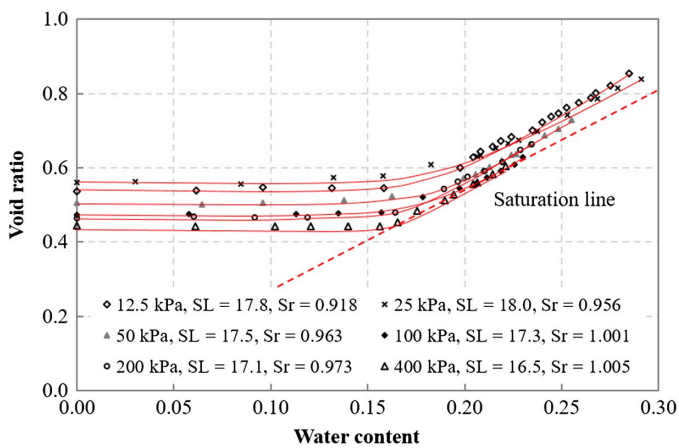

0.4 to 0.9, as shown in Fig. 9. For the tested soil mixture, with the volume measurement accuracy of 0.35 % obtained from the evaluation test on the aluminum cylinders, the corresponding accuracy of the void ratio measurement was determined to be 0.0049 to 0.0067, which is considered acceptable for shrinkage curve measurement. For a specific soil specimen, each volume measurement using the photogrammetric method was independent from the other measurements. As a result, the smoothness of the shrinkage curves, as shown in Fig. 9, indicated that the measurement accuracy of the photogrammetric method is reliable for soil shrinkage curve measurement.

Discussions

For a shrinkage test, the soil specimen is considered a representative soil element. In order to be considered an element, the soil deformation during drying is supposed to be uniform. As a result, a soil specimen with cracks cannot be considered a soil element because it is not a representative soil element, because of the nonuniform deformation history. However, for cohesive soils, especially expansive soils, the soil usually cracks during continuous drying, because of nonuniform deformation. For the proposed method, to avoid cracking during drying, a container/cap could be used to cover the soil specimen after being exposed to the atmosphere for a certain time (e.g., 15 minutes) to slow down the drying process and allow water redistribution in the soil. In this way, the moisture in the soil was more evenly distributed when compared to the soils during continuous drying. This crack control technique was previously verified in Zhang (2004). As a result, the cracking problem is not a concern for the proposed shrinkage curve measurement method.

Even though the proposed method aims at measuring the shrinkage curves of soil samples without cracks, when there is a need, the proposed method can definitely be used to measure the soil volume through reconstructing the cracked soil surface. A typical example is presented in Fig. 10 to demonstrate the performance of the proposed volume measurement method for the surface reconstruction of a soil specimen with a purposely made crack, as shown in Fig. 10a. With the proposed method, the 3D soil surface was reconstructed. Fig. 10b shows the soil surface colored from the height of the specimen, from which the crack, as shown in Fig. 10a, could be easily identified. This crack is also clearly shown on the reconstructed surfaces, shown in Fig. 10c and d, viewed at different angles. As a result, with this constructed soil surface, this crack in the soil could be taken into consideration when measuring the soil volume.

As previously discussed, for the shrinkage curve measurement method proposed by Sander and Gerke (2007), to reconstruct the 3D model of the soil clod, some erratic points must be removed. The removal of erratic points was subjective. When compared to the method proposed in this article, these erratic points could be easily removed through a comparison between the picture, typically as shown in Fig. 10a, and the reconstructed soil surface, typically as shown in Fig. 10c.

Similar to the other shrinkage curve measurement methods, the proposed method cannot be used to measure the shrinkage curve of soils under loading condition either. However, this does not necessarily mean that the shrinkage curve of soils under loading condition cannot be measured. The following two options can potentially be utilized to achieve this purpose: (1) modifying the conventional one-dimensional consolidation cell by adopting the axis-translation technique to control soil suction during drying. A change in soil suction corresponds to a soil water content change. During the drying

FIG. 10

Reconstructed soil surface with a purposely made crack.

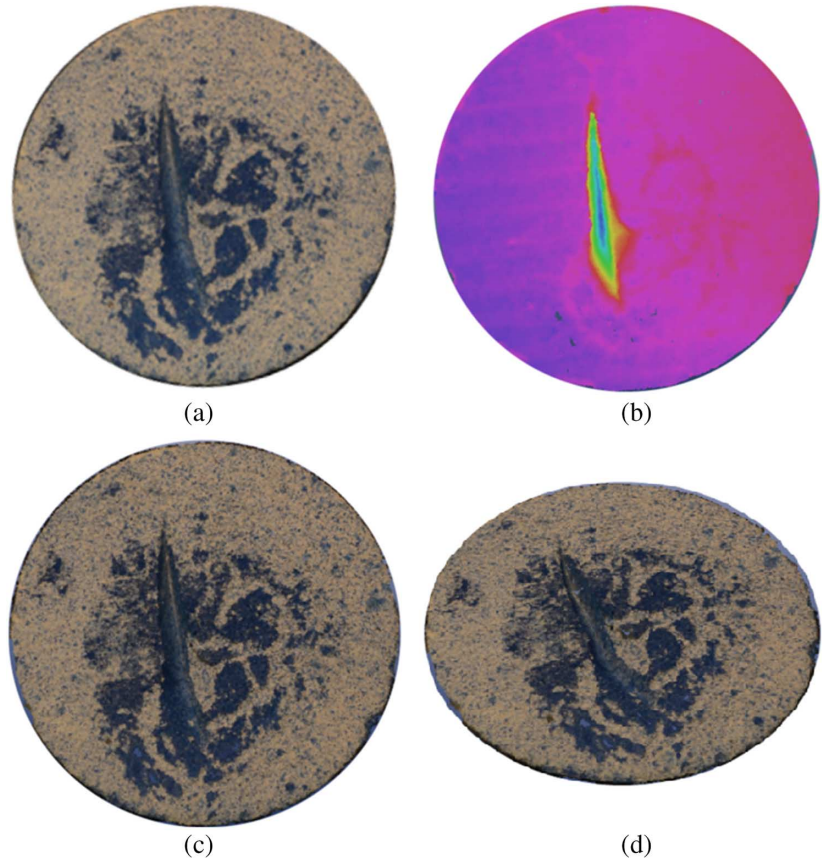

process, the soil water content and volume during loading can be measured by monitoring the amount of water out of the soil and a linear variable differential transformer mounted at the top of the soil, respectively. (2) Using the suction-controlled triaxial test apparatus (e.g., Bishop and Donald 1961) or modifying the conventional triaxial cell by adopting the axis-translation technique to control the soil suction and the newly developed photogrammetry-based method (Zhang et al. 2015; Li et al. 2016; and Li and Zhang 2015a) to measure the soil volume change during testing. In this method, the soil water content change is also obtained through monitoring the water expelled out of the soil during the suction control process. For these methods, the soils are tested under the K0 and triaxial loading conditions, respectively.

The volume measurement accuracy is critical for an accurate shrinkage curve measurement. It is worth noting that the soils used in the previous evaluation tests are a mixture of Fairbanks silt and Kaolin at a ratio of 1:1. Kaolin itself is a low plasticity soil. When mixed with Fairbanks silt at a ratio of 1:1, the plasticity index of the soil mixture is 5.8, which indicates that its swelling/shrinking potential is even lower. **Fig. 9** demonstrates that the accuracy of the proposed method is high enough to obtain reasonable results even for soils with low swelling/shrinking potential. In addition, larger samples are recommended for soils with extremely low shrinking potential.

Conclusions

This study proposed a new method to measure soil shrinkage curves. The soil water content and volume change during drying were measured using a digital balance and a photogrammetric technique, respectively. Using the photogrammetric technique, a point cloud that represented the detailed 3D soil surface could be reconstructed. With the obtained 3D point cloud, a triangular mesh was then generated for accurate soil volume calculation. The nonuniform soil deformation during drying could be taken into consideration when measuring the soil volume. The error of the volume measurement method was evaluated to be 0.35 % and 0.43 % through tests on aluminum cylinders and a saturated soil, respectively. A series of shrinkage tests were also conducted on a soil mixture. Test results indicated that the proposed method was reliable and efficient for shrinkage curve measurement when compared to the other methods.

References

Adrian, R. J., 1991, "Particle-Imaging Techniques for Experimental Fluid Mechanics," *Annu. Rev. Fluid Mech.*, Vol. 23, No. 1, pp. 261–304, https://doi.org/10.1146/annurev.fl.23.010191.001401

ASTM D427-04, 2004, *Standard Test Method for Shrinkage Factors of Soils by the Mercury Method*, ASTM International, West Conshohocken, PA, www.astm.org

ASTM D4943-08, 2008, *Standard Test Method for Shrinkage Factors of Soils by the Wax Method*, ASTM International, West Conshohocken, PA, www.astm.org

Bensallam, S., Bahi, L., Ejjaaouani, H., and Shakhirev, V., 2012, "Shrinkage Curve: Experimental Study and Modelling," *Int. J. Eng.*, Vol. 25, No. 3, pp. 203–210, https://doi.org/10.5829/idosi.ije.2012.25.03a.02

Berndt, R. D. and Coughlan, K. J., 1977, "The Nature of Changes in Bulk Density with Water Content in a Cracking Clay," *Soil Res.*, Vol. 15, No. 1, pp. 27–37, https://doi.org/10.1071/SR9770027

Bhandari, A. R., Powrie, W., and Harkness, R. M., 2012, "A Digital Image-Based Deformation Measurement System for Triaxial Tests," *Geotech. Test. J.*, Vol. 35, No. 2, pp. 209–226, https://doi.org/10.1520/GTJ103821

Bishop, A. W. and Donald, I. B., 1961, "The Experimental Study of Partly Saturated Soil in the Triaxial Apparatus," presented at the *Fifth International Conference on Soil Mechanics and Foundation Engineering*, Paris, France, Dunod, Paris, France, pp. 13–21.

Boivin, P., 2007, "Anisotropy, Cracking, and Shrinkage of Vertisol Samples Experimental Study and Shrinkage Modeling," *Geoderma*, Vol. 138, Nos. 1–2, pp. 25–38, https://doi.org/10.1016/j.geoderma.2006.10.009

Brasher, B. R., Franzmeier, D. P., Valassis, V., and Davidson, S. E., 1966, "Use of Saran Resin to Coat Natural Soil Clods for Bulk-Density and Water-Retention Measurements," *Soil Sci.*, Vol. 101, No. 2, 108p, https://doi.org/10.1097/00010694-196602000-00006

Braudeau, E., Costantini, J. M., Bellier, G., and Colleuille, H., 1999, "New Device and Method for Soil Shrinkage Curve Measurement and Characterization," *Soil Sci. Soc. Am. J.*, Vol. 63, No. 3, pp. 525–535, https://doi.org/10.2136/sssaj1999.03615995006300030015x

Bronswijk, J. J. B., 1990, "Shrinkage Geometry of a Heavy Clay Soil at Various Stresses," *Soil Sci. Soc. Am. J.*, Vol. 54, No. 5, pp. 1500–1502, https://doi.org/10.2136/sssaj1990.03615995005400050048x

Cornelis, W. M., Corluy, J., Medina, H., Díaz, J., Hartmann, R., Van Meirvenne, M., and Ruiz, M. E., 2006, "Measuring and Modelling the Soil Shrinkage Characteristic Curve," *Geoderma*, Vol. 137, Nos. 1–2, pp. 179–191, https://doi.org/10.1016/j.geoderma.2006.08.022

Crescimanno, G. and Provenzano, G., 1999, "Soil Shrinkage Characteristic Curve in Clay Soils: Measurement and Prediction," *Soil Sci. Soc. Am. J.*, Vol. 63, No. 1, pp. 25–32, https://doi.org/10.2136/sssaj1999.03615995006300010005x

Fredlund, D. G. and Houston, S. L., 2013, "Interpretation of Soil-Water Characteristic Curves When Volume Change Occurs as Soil Suction is Changed," *Advances in Unsaturated Soils*, CRC Press, Boca Raton, FL, pp. 15–31.

Fredlund, D. G. and Zhang, F., 2013, "Combination of Shrinkage Curve and Soil-Water Characteristic Curves for Soils that Undergo Volume Change as Soil Suction is Increased," presented at the *18th International Conference on Soil Mechanics and Geotechnical Engineering*, Paris, France, International Society for Soil Mechanics and Geotechnical Engineering, London, UK, pp. 1109–1112.

Helm, J. D., McNeill, S. R., and Sutton, M. A., 1996, "Improved 3D Image Correlation for Surface Displacement Measurement," *Opt. Eng.*, Vol. 35, No. 7, pp. 1911–1920, https://doi.org/10.1117/1.600624

Hobbs, P. R. N., Jones, L. D., Kirkham, M. P., Roberts, P., Haslam, E. P., and Gunn, D. A., 2014, "A New Apparatus for Determining the Shrinkage Limit of Clay Soils," *Géotechnique*, Vol. 64, No. 3, pp. 195–203, https://doi.org/10.1680/geot.13.P.076

Huang, C., Shao, M., and Tan, W., 2011, "Soil Shrinkage and Hydrostructural Characteristics of Three Swelling Soils in Shaanxi, China," *J. Soils Sediments*, Vol. 11, No. 3, pp. 474–481, https://doi.org/10.1007/s11368-011-0333-8

Jain, S., Wang, Y. H., and Fredlund, D. G., 2015, "Non-Contact Sensing System to Measure Specimen Volume During Shrinkage Test," *Geotech. Test. J.*, Vol. 38, No. 6, pp. 1–14, https://doi.org/10.1520/GTJ20140274

Kim, D. J., Vereecken, H., Feyen, J., Boels, D., and Bronswijk, J. J. B., 1992, "On the Characterization of Properties of an Unripe Marine Clay Soil: I. Shrinkage Processes of an Unripe Marine Clay Soil in Relation to Physical Ripening," *Soil Sci.*, Vol. 153, No. 6, pp. 471–481, https://doi.org/10.1097/00010694-199206000-00006

Krosley, L., Likos, W. J., and Lu, N., 2003, "Alternative Encasement Materials for the CLOD Test," *Geotech. Test. J.*, Vol. 26, No. 4, pp. 461–463, https://doi.org/10.1520/GTJ11259J

Li, L. and Zhang, X., 2015a, "A New Triaxial Testing System for Unsaturated Soil Characterization," *Geotech. Test. J.*, Vol. 38, No. 6, pp. 823–839, https://doi.org/10.1520/GTJ20140201

Li, L. and Zhang, X., 2015b, "Modified Unconfined Compression Testing System to Characterize Stress–Strain Behavior of Unsaturated Soils at Low Confining Stresses," *Trans. Res. Rec. J. Trans. Res. Board*, Vol. 2510, pp. 54–64, https://doi.org/10.3141/2510-07

Li, L., Zhang, X., Chen, G., and Lytton, R., 2016, "Measuring Unsaturated Soil Deformations during Triaxial Testing Using a Photogrammetry-Based Method," *Can. Geotech. J.*, Vol. 53, No. 3, pp. 472–489, https://doi.org/10.1139/cgj-2015-0038

Lin, H. and Penumadu, D., 2006, "Strain Localization in Combined Axial-Torsional Testing on Kaolin Clay," *J. Eng. Mech.*, Vol. 132, No. 5, pp. 555–564, https://doi.org/10.1061/(ASCE)0733-9399(2006)132:5(555)

Lu, N. and Kaya, M., 2013, "A Drying Cake Method for Measuring Suction-Stress Characteristic Curve, Soil–Water-Retention Curve, and Hydraulic Conductivity Function," *Geotech. Test. J.*, Vol. 36, No. 1, pp. 1–19, https://doi.org/10.1520/GTJ20120097

McGarry, D. and Daniells, I. G., 1987, "Shrinkage Curve Indices to Quantify Cultivation Effects on Soil Structure of a Vertisol," *Soil Sci. Soc. Am. J.*, Vol. 51, No. 6, pp. 1575–1580, https://doi.org/10.2136/sssaj1987.03615995005100060031x

Merel, A. P. and Farres, P. J., 1998, "The Monitoring of Soil Surface Development Using Analytical Photogrammetry," *Photogramm. Rec.*, Vol. 16, No. 92, pp. 331–345, https://doi.org/10.1111/0031-868X.00129

Mikhail, E. M., Bethel, J. S., and McGlone, J. C., 2001, *Introduction to Modern Photogrammetry*, John Wiley & Sons, Inc., Hoboken, NJ, 496p.

Puppala, A. J., Katha, B., and Hoyos, L. R., 2004, "Volumetric Shrinkage Strain Measurements in Expansive Soils Using Digital Imaging Technology," *Geotech. Test. J.*, Vol. 27, No. 6, pp. 547–556, https://doi.org/10.1520/GTJ12069

Puppala, A. J., Manosuthikij, T., and Chittoori, B. C., 2013, "Swell and Shrinkage Characterizations of Unsaturated Expansive Clays from Texas," *Eng. Geol.*, Vol. 164, pp. 187–194, https://doi.org/10.1016/j.enggeo.2013.07.001

Rechenmacher, A. L. and Medina-Cetina, Z., 2007, "Calibration of Soil Constitutive Models with Spatially Varying Parameters," *J. Geotech. Geoenviron. Eng.*, Vol. 133, No. 12, pp. 1567–1576, https://doi.org/10.1061/(ASCE)1090-0241(2007)133:12(1567)

Reeve, M. J., Hall, D. G. M., and Bullock, P., 1980, "The Effect of Soil Composition and Environmental Factors on the Shrinkage of Some Clayey British Soils," *J. Soil Sci.*, Vol. 31, No. 3, pp. 429–442, https://doi.org/10.1111/j.1365-2389.1980.tb02092.x

Sachan, A. and Penumadu, D., 2007, "Strain Localization in Solid Cylindrical Clay Specimens Using Digital Image Analysis (DIA) Technique," *Soils Found.*, Vol. 47, No. 1, pp. 67–78, https://doi.org/10.3208/sandf.47.67

Sander, T. and Gerke, H. H., 2007, "Noncontact Shrinkage Curve Determination for Soil Clods and Aggregates by Three-Dimensional Optical Scanning," *Soil Sci. Soc. Am. J.*, Vol. 71, No. 5, pp. 1448–1454, https://doi.org/10.2136/sssaj2006.0372

Schafer, W. M. and Singer, M. J., 1976, "A New Method of Measuring Shrink-Swell Potential Using Soil Pastes," *Soil Sci. Soc. Am. J.*, Vol. 40, No. 5, pp. 805–806, https://doi.org/10.2136/sssaj1976.03615995004000050050x

Sibley, J. and Williams, D., 1989, "A Procedure for Determining Volumetric Shrinkage of an Unsaturated Soil," *Geotech. Test. J.*, Vol. 12, No. 3, pp. 181–187, https://doi.org/10.1520/GTJ10966J

Stewart, R. D., Abou Najm, M. R., Rupp, D. E., and Selker, J. S., 2012, "An Image-Based Method for Determining Bulk Density and the Soil Shrinkage Curve," *Soil Sci. Soc. Am. J.*, Vol. 76, No. 4, pp. 1217–1221, https://doi.org/10.2136/sssaj2011.0276n

Sutton, M. A., McNeill, S. R., Helm, J. D., and Chao, Y. J., 2000, "Advances in Two-Dimensional and Three-Dimensional Computer Vision," *Photomechanics*, Vol. 77, pp. 323–372.

Tariq, A.-U.-R. and Durnford, D. S., 1993, "Soil Volumetric Shrinkage Measurements: A Simple Method," *Soil Sci.*, Vol. 155, No. 5, pp. 325–330, https://doi.org/10.1097/00010694-199305000-00003

Triggs, B., McLauchlan, P. F., Hartley, R. I., and Fitzgibbon, A. W., 2000, "Bundle Adjustment – A Modern Synthesis," presented at the *International Conference on Computer Vision*, Kerkyra, Corfu, Greece, Institute of Electrical and Electronics Engineers Computer Society, Washington, DC, pp. 298–375.

White, D. J., Take, W. A., and Bolton, M. D., 2003, "Soil Deformation Measurement Using Particle Image Velocimetry (PIV) and Photogrammetry," *Géotechnique*, Vol. 53, No. 7, pp. 619–632, https://doi.org/10.1680/geot.2003.53.7.619

Zhang, X., 2004, "Consolidation Theories for Saturated-Unsaturated Soils and Numerical Simulation of Residential Buildings on Expansive Soils," Ph.D. dissertation, Texas A&M University, College Station, TX.

Zhang, X., Li, L., Chen, G., and Lytton, R., 2015, "A Photogrammetry-Based Method to Measure Total and Local Volume Changes of Unsaturated Soils during Triaxial Testing," *Acta Geotech*, Vol. 10, No. 1, pp. 55–82, https://doi.org/10.1007/s11440-014-0346-8